Resonant tunneling in small current-biased Josephson junctions

J. M. Schmidt, A. N. Cleland, and John Clarke
Department of Physics, University of California, Berkeley, California 94720
and Materials Sciences Division, Lawrence Berkeley Laboratory, Berkeley, California 94720
(Received 26 July 1990; revised manuscript received 24 September 1990)

We investigate the theory of resonant tunneling of the phase difference ϕ in current-biased, small-capacitance Josephson junctions. Tunneling of ϕ occurs between states localized in adjacent wells of the tilted cosine ("washboard") potential when the states are nearly degenerate, and leads to unique junction behavior. Most notable are the presence of voltage spikes along the supercurrent branch of the current-voltage characteristic, the reduction of the bias current at which the junction switches to the free-running state to a value well below the thermodynamic value, and peaks in the distribution of rates at which this switching occurs as a function of bias current. For a range of junction parameters, we estimate the magnitude and width of the first (lowest bias current) voltage spike and the rate of switching to the free-running state in the zero temperature, low damping limit. Experimentally, the most readily observable signature of resonant tunneling should be the characteristic peaks in the switching distribution.

I. INTRODUCTION

In exploring the validity of the application of quantum mechanics to macroscopic systems,[1] one often chooses the current-biased Josephson junction as a system to study, both theoretically and experimentally. The phase difference ϕ between the superconducting condensates in the electrodes obeys an equation of motion identical to that of a particle moving in a cosine potential that is tilted in proportion to the bias current.[2] For bias currents below the critical current of the junction, this "tilted washboard" potential consists of a set of wells in which the particle can be trapped, whereas above the critical current the particle can move freely down the potential. Treating this macroscopic system quantum mechanically, we expect to find distinctly nonclassical features, two of which already have been verified experimentally. One is the existence of quasibound states in the wells with discrete energy levels,[3] demonstrated with microwave-spectroscopy techniques. The other is the macroscopic quantum tunneling of the particle from one of these bound states into the continuous spectrum of free-running states.[3–7]

The possibility of a third quantum-mechanical process occurring within this system has been suggested,[8,9] namely the quantum tunneling from one of the bound states of a potential well into another bound state in an adjacent well. This process, called resonant tunneling, occurs when the bias current is such that the ground-state energy of one well is equal to the energy of an excited state in the adjacent well. The tunneling between the two states is coherent; when the system is prepared in one of the states which are not eigenstates of the Hamiltonian, it will oscillate in time between the two. This is analogous to the well-known ammonia molecule resonance and to the predicted macroscopic quantum coherent superposition of states of an rf superconducting quantum interference device (SQUID).[1] One important distinction between the case of the SQUID and the problem at hand is that in the former case the resonance studied is between two local ground states, whereas in the latter case one of the states is excited.

Once the system has undergone a resonant tunneling transition to an excited state, it can either decay to a lower state or continue to tunnel. These competing processes each lead to observably distinct results in the behavior of the junction. If, after tunneling to the excited state, the system decays to the local ground state, the entire process may repeat, resulting in the movement of the particle from well to well down the potential (path A in Fig. 1). Because this motion corresponds to a nonzero voltage across the junction, we expect that the resonant tunneling process will be reflected in the supercurrent portion of the current-voltage characteristics as a series of voltage spikes [Fig. 2(a)], each spike corresponding to an aligned pair of states. This structure is unusual in that it can occur for bias currents which are much less than

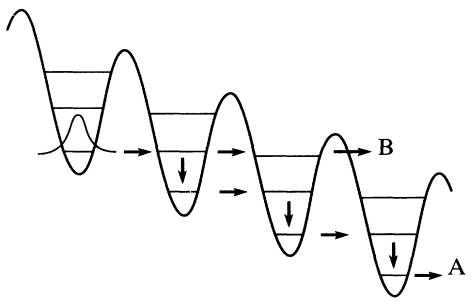

FIG. 1. Two possible transition paths for the particle started in a ground state. Motion along path A, an alternating sequence of resonant tunneling and decay transitions, results in steady phase slips. Motion along path B, which is a sequence of successive resonant tunneling transitions, results in escape to the free-running state.

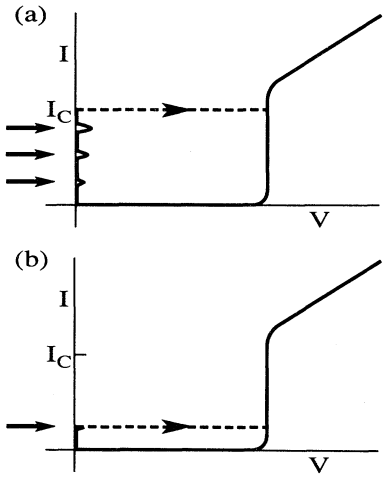

FIG. 2. Schematic representations of the current-voltage characteristic: (a) steady phase slips (path A in Fig. 1) result in voltage peaks along the supercurrent branch which correspond to the alignment of energy levels; (b) escape (path B in Fig. 1) results in a switching current greatly reduced from the Ambegaokar-Baratoff (Ref. 15) critical current I_C. These features are indicated by arrows.

the critical current. This macroscopic process is similar to that occurring in semiconductor superlattices at the microscopic level,[10] where increases in conductivity are observed when a strong electric field brings electronic energy levels of adjacent wells into alignment. In contrast to the process of sequential tunneling and decay, additional resonant tunneling events occurring before the decay to the ground state could lead eventually to the transition of the system to the free running state (path B in Fig. 1), thereby destroying the spike structure. Here one should instead observe a switching of the junction from the supercurrent branch to the quasiparticle branch at a value of bias current below the thermodynamic critical current [Fig. 2(b)].

Resonant tunneling in a Josephson junction is of interest not only as a novel phenomenon in its own right, but also because of its possible effect on the coherent Bloch oscillations predicted to occur in small capacitance junctions.[11] It has been suggested[12] that for values of bias current in the vicinity of the resonances the resonant tunneling transition to excited states will break the coherence of the Bloch oscillations. The importance of the resonant tunneling transition was also noted by Kondo,[13] who, in order to examine the suppression of Bloch oscillations by Zener tunneling, numerically integrated the Schrödinger equation for this system. The wave functions he obtained explicitly show the resonance, although the dynamics of the resonant transition were not investigated in that work.

Other authors have undertaken theoretical studies of the resonant tunneling phenomenon in Josephson junctions. However, the early studies[9,14] had not comprehensively taken into account all the features of the problem which we believe to be important. Most notable among these are the coherence of the tunneling, and the competition between decay and successive tunneling. The coherence of the transition from one bound state to another must be included because the probability of return tunneling is not necessarily negligible, implying that Fermi's golden rule may be invalid in some situations. Although decay and successive tunneling rates are directly compared in Ref. 14, we believe that these quantities require a more detailed consideration within the context of the dynamics of the system. During the completion of this work we became aware of the recent results of Zhuravlev and Zorin,[15] who employed a similar approach to ours that includes the coherence of the resonant tunneling transition. However, they did not estimate the energies of the states in the wells beyond a harmonic approximation, and the corrections for the anharmonicity of the potential have important implications for the dynamics.

The purpose of the present work is to carry out an investigation in order to determine which effects due to resonant tunneling are observable experimentally, if any. We estimate the magnitude, width, and duration of the voltage peak developed before the junction switches to the normal state, and the rate at which this switching occurs. These quantities are computed for a range of junction parameters. From our results we conclude that the most readily observable signature of resonant tunneling in a Josephson junction is not the voltage peaks, but rather the unique distribution of rates at which the junction switches to the normal state. This distribution is nonmonotonic in the bias current, exhibiting peaks at values of current corresponding to resonances.

Our approach is as follows. The analysis is for zero temperature, and we consider the effects of dissipation only to supply a decay mechanism, neglecting its effect on tunneling rates.[16] Using a perturbative technique, we calculate the energy levels of the quasibound states, starting with a harmonic approximation in each well. We use the WKB method to estimate the coupling between states in adjacent wells and the tunneling rate to the free running states. We then use a density-matrix approach to investigate the motion of the system when the junction is biased at or near resonance. In this way we are able to include both coherent and incoherent transitions in a comprehensive manner.

II. HARMONIC-OSCILLATOR APPROXIMATION AND PERTURBATIVE SOLUTIONS

A. Multiple harmonic wells approximation

The Hamiltonian describing the resistively shunted junction model of a Josephson junction in the limit of infinite resistance is given by[8]

$$\tilde{H}=-4E_C\frac{d^2}{d\phi^2}-E_J\cos\phi-\frac{I}{I_C}E_J\phi\ , \tag{1}$$

where $E_C=e^2/2C$ is the charging energy for a junction of capacitance C, I is the bias current, I_C is the critical current given by the Ambegaokar and Baratoff relation,[17] and $E_J=\hbar I_C/2e$ is the Josephson coupling energy. This

is also the Hamiltonian for a particle moving in the tilted washboard potential. Focusing on the well located at the origin, one can separate $\tilde{H}$ into harmonic and anharmonic parts by writing

$$\tilde{H}=\tilde{H}^0_{\rm SHO}+\Delta\tilde{H} \ , \tag{2}$$

where $\tilde{H}^0_{\rm SHO}$ is the Hamiltonian for the simple harmonic oscillator,

$$\tilde{H}^0_{\rm SHO}=-4E_C\frac{d^2}{d\phi^2}+\frac{E_J}{2}\phi^2-E_J \ , \tag{3}$$

and $\Delta\tilde{H}$ contains the term linear in ϕ together with quartic and higher-order terms. If the eigenfunctions of $\tilde{H}^0_{\rm SHO}$ are sufficiently localized, the harmonic Hamiltonian will allow us to obtain approximate solutions for the energies of the states localized in this well of the washboard potential, and we may consider $\Delta\tilde{H}$ as a perturbation to $\tilde{H}^0_{\rm SHO}$.

For ease of algebraic manipulation we define the parameter $\nu=\sqrt{E_J/2E_C}$ and let $\phi=x\sqrt{2/\nu}$. Physically, ν corresponds roughly to the number of levels in the well. In addition, we choose the energy unit to be the zero-point energy of the oscillator $\sqrt{2E_CE_J}=\hbar\omega_p/2$ (ω_p is 2π times the plasma frequency). We thus obtain (dropping the tilde in these units)

$$H^0_{\rm SHO}=-\frac{d^2}{dx^2}+x^2-\nu \ , \tag{4}$$

which has the energy spectrum

$$E^0_m=-\nu+2m+1, \quad m=0,1,2,\ldots \ . \tag{5}$$

In these units, the full Hamiltonian (1) is given by

$$H=-\frac{d^2}{dx^2}+V(x) \ , \tag{6a}$$

where $V(x)$ is the potential

$$V(x)=-\nu\cos(x\sqrt{2/\nu})-sx\sqrt{2\nu} \ , \tag{6b}$$

and $s=I/I_C$. The energy spectrum of H forms a Wannier-Stark ladder. Thus, given the levels E_m located in a particular well, we can generate the full set of levels

$$F_{n,m}=E_m-2\pi s\nu n \ , \tag{7}$$

where n is the integer which labels the nth well. If we take E^0_m as an approximation to the actual levels E_m, we see that at particular values of bias current $I=I^{\rm res}_m$ the ground state of the nth well is degenerate with the mth state of the $(n+1)$th well; that is,

$$F_{n,0}=F_{n+1,m} \ , \tag{8}$$

when

$$I^{\rm res}_m=I_C\frac{m}{\pi\nu}=m\frac{e}{\pi}\omega_p \ . \tag{9}$$

This is the condition for resonance obtained previously.[8,9,12] Note that in this approximation the resonance peaks will be equally spaced along the current axis. Also, we see the degeneracies which occur at resonance are multiple. For example, at $I=I^{\rm res}_m$, $F_{n+1,m}=F_{n+2,2m}$ in addition to the degeneracy given by Eq. (8), and so on. This implies that successive resonant tunneling events may be an important transition sequence, and we must investigate to what extent these additional degeneracies are removed by the inclusion of corrections to $F_{n,m}$.

B. Energy-level corrections

We wish to calculate the corrections $\Delta E_m=E_m-E^0_m$ for the energy levels which appear upon inclusion of the anharmonic perturbation ΔH. These corrections can be obtained using time-independent perturbation theory with harmonic-oscillator eigenfunctions as a basis, and the results expanded as a power series in $1/\nu$. This assumes that the coupling to the states in adjacent wells is negligible, which we shall see later is justified.

To obtain corrections of order ν^{-2} one must carry the linear term in ΔH to fourth order in a perturbation expansion, noting that s is of order ν^{-1} at resonance. This is unnecessarily tedious; instead we expand the potential about the minimum of the 0th well, which is located at $x_0=\sqrt{\nu/2}\sin^{-1}s$. Letting $x=x_0+\Delta x$, we can write Eq. (6) as

$$H=H^2_{\rm SHO}+H_s+H_a \ , \tag{10a}$$

where

$$H^2_{\rm SHO}=-\frac{d^2}{d\Delta x^2}+(1-s^2)^{1/2}[-\nu+(\Delta x)^2]-s\nu\sin^{-1}s \ , \tag{10b}$$

$$H_s=(1-s^2)^{1/2}[\nu-(\Delta x)^2-\nu\cos(\Delta x\sqrt{2/\nu})] \ , \tag{10c}$$

and

$$H_a=s\nu[\sin(\Delta x\sqrt{2/\nu})-\Delta x\sqrt{2/\nu}] \ . \tag{10d}$$

Since H_s is of order ν^{-1}, it must be carried to second order. On the other hand, H_a is of order $\nu^{-3/2}$ and need only be retained to first order, and its contribution vanishes by parity. We can now recombine $H^2_{\rm SHO}$ and H_s; the resulting Schrödinger equation takes the form of Mathieu's differential equation. Using the asymptotic expansion for the characteristic values of this equation,[18] we obtain to second order in $1/\nu$

$$\Delta E_m=-\frac{\nu s^2}{2}-\frac{ws^2}{4}-\frac{w^2+1}{16\nu}-\frac{w^3+3w}{256\nu^2} \ , \tag{11}$$

where $w=2m+1$.

The dependence of ΔE_m on m shows the levels E_m are not evenly spaced, which means degeneracies only occur in pairs for a given bias current. This will have important consequences for the dynamics for it will tend to suppress sequential resonant tunneling events, as we will see later. By including this correction to the energy levels and using Eq. (8) we can obtain the value of the bias current at resonance to second order in $1/\nu$,

$$I^{\rm res}_m=m\frac{e}{\pi}\omega_p\left[1-\frac{m+1}{8\nu}-\frac{m^2}{4\pi^2\nu^2}-\frac{2m^2+3m+3}{128\nu^2}\right] . \tag{12}$$

We note that because of the anharmonicity of the potential the resonance peaks are not evenly spaced along the current axis.

C. Coupling between wells

Next we consider the coupling between states of different wells. We estimate the matrix elements $H_{n,m,n',m'}$ when the states are degenerate, that is $F_{n,m}=F_{n',m'}$. We assume nearest-neighbor coupling only, so that $H_{n,m,n',m'}=0$ for $|n-n'|>1$. For $n'-n=1$, we use the WKB method to extend the harmonic-oscillator wave functions into the region under the barrier. With these semiclassical wave functions we obtain estimates of the matrix elements, which are independent of n and are given by

$$H_{0,m,1,m'}=\frac{1}{\pi}\sqrt{G(m)G(m')}\exp(-I_m)\ , \tag{13}$$

where

$$I_m=\int_{x_m^-}^{x_m^+}[V(x')-E_m]^{1/2}\,dx'\ . \tag{14}$$

The limits of the integral are the classical turning points where the integrand is zero, and V and E_m are evaluated at the bias current where $F_{0,m}=F_{1,m'}$. The dimensionless parameter $G(m)$ is of order unity and depends weakly on the level index m,

$$G(m)=\frac{\pi^{1/2}}{2^m\,m!}\left[\frac{2m+1}{e}\right]^{m+1/2}\ . \tag{15}$$

We note that the coupling decreases exponentially with the barrier height. The coupling is quite small for values of ν of interest ($\nu\gtrsim 2$), which justifies our earlier assumption that the interwell coupling is weak.

III. DYNAMICS

A. General considerations

Having determined the matrix elements of the Hamiltonian in the basis of states localized in the wells, we are now equipped to study the motion of the system. In particular, we wish to answer two questions: What is the average rate of motion of the particle down the washboard, and how long will this motion persist before the particle undergoes a transition to a free running state? The average rate of motion determines the voltage across the junction before it switches to the normal state, and the lifetime of the process determines the time during which we have to measure this voltage and the distribution of rates at which the junction switches.

We restrict our analysis to the case of the bias current I set at or near its first resonance value $I_1^{\rm res}$. Here the system consists of a set of bound states which can be subdivided into groups of $l_{\rm max}$ degenerate or nearly degenerate states, where $l_{\rm max}$ is the number of bound states in a well, and each state in a group is from a different well. For convenience, we label states in the kth group, or subsystem, as Ψ_{kl}, where $k=n-m$ and $l=m+1$ with $k=\ldots,-2,-1,0,1,2,\ldots$ and $l=1,2,\ldots,l_{\rm max}$ (see Fig. 3).

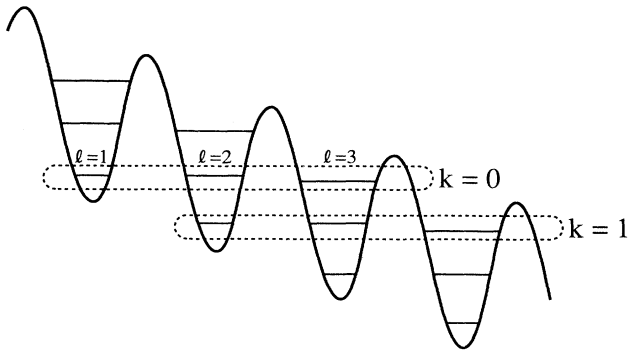

FIG. 3. Subsystems for $l_{\rm max}=3$ (three states per subsystem). The subsystems for $k=0$ and 1 are each enclosed by the dashed oval.

Within one of these subsystems the states Ψ_{kl} are no longer eigenstates, but are mixed because of the nonzero coupling between them. This results in coherent motion among states Ψ_{kl} with the same k when the subsystem is started in one of them. In addition to this coherent motion within a subsystem, two types of incoherent transitions out of the subsystem are possible. One is the decay to a state in a lower subsystem leading to motion down the washboard, and the other is the tunneling from a state $\Psi_{kl_{\rm max}}$ to the continuum of free running states, resulting in the junction switching into the normal state. As we perform this calculation in the zero-temperature limit, we do not consider thermally induced transitions.

In light of the above, we adopt the following general method of solution: We associate with each subsystem k its density matrix ρ^k, which is of dimension $l_{\rm max}\times l_{\rm max}$, and examine the equations of motion for the entire set of density matrices. Each of these contains terms associated with the coherent motion within that subsystem, and terms representing the incoherent coupling to other subsystems and the set of free running states.

B. Resonant tunneling peak magnitude and shape

First we investigate the motion of the system which leads to peak structure on the supercurrent branch of the current-voltage characteristic, shows as path A in Fig. 1. The states involved in this motion are Ψ_{k1} and Ψ_{k2} with $k=0,1,2,\ldots$. Here we exclude the effects of additional states Ψ_{kl} with $l>2$, and ignore the possibility of escape. We shall see later that in the cases where the peak structure has a significant lifetime these result only in a small perturbation to the overall motion down the potential; in addition the general method is most clearly illustrated in this simple case and can be extended to include escape in a straightforward way.

Coherent motion within the kth subsystem is described by the matrix representation H_0 of the Hamiltonian in the basis $\{\Psi_{k1},\Psi_{k2}\}$. Before being coupled, these states differ in energy by an amount σ, which to lowest order in $1/\nu$ depends on the bias current as

$$\sigma=2\pi\nu(I-I_1^{\rm res})I_C\ . \tag{16}$$

Taking the reference energy to be halfway between these energies, we have

$$H_0=\begin{bmatrix} \frac{\sigma}{2} & \frac{\Delta_1}{2} \\ \frac{\Delta_1}{2} & \frac{-\sigma}{2} \end{bmatrix}, \tag{17}$$

where we have defined $\Delta_1/2 \equiv H_{0,0,1,1}$ for brevity in notation.

The decay of a state Ψ_{k2} to $\Psi_{k+1,1}$ is induced by terms which are not included in the present Hamiltonian. However, we may include the decay phenomenologically by adding an imaginary term $-i\Gamma_d/2$ (again in units of $\hbar\omega_p/2$) to the energy of state Ψ_{k2}; this results in a characteristic decay rate of $\omega_p\Gamma_d/2$. To obtain an order-of-magnitude estimate of Γ_d we apply the results of Esteve, Devoret, and Martinis,[19] who calculated the complex energy shifts for a Josephson junction with a parallel external circuit consisting of an ohmic resistor R. They found that Γ_d is given roughly by $\Gamma_d \cong 2/Q$, where $Q=RC\omega_p$ is the classical quality factor, assumed to be much larger than unity. The imaginary terms representing decay can be added to the representation of the Hamiltonian as the matrix $-i\Gamma/2$, where

$$\Gamma=\begin{bmatrix} 0 & 0 \\ 0 & \Gamma_d \end{bmatrix}. \tag{18}$$

Now suppose that the particle is localized in state Ψ_{01} at time $t=0$. The usual equation of motion for the density matrix ρ^0 of dimension 2×2 of the $k=0$ subsystem is modified by the presence of imaginary energy terms; it is now

$$\frac{d}{d\tau}\rho^0=-i[H_0,\rho^0]-\tfrac{1}{2}[\Gamma,\rho^0]_+ , \tag{19}$$

where the differentiation is carried out with respect to the dimensionless time variable $\tau=\omega_p t/2$. Equation (19) can be solved analytically. The result shows the trace of ρ^0 is not conserved: probability density leaves the $k=0$ subsystem because of the imaginary energy terms.

Consider next the subsystems with $k>0$. The probability density leaving a particular subsystem $k-1$ enters the subsystem k incoherently in the state $\Psi_{k,1}$, where it again begins coherent motion and further decay. We thus include a source term in each of the equations of motion for these subsystems, which become

$$\frac{d}{d\tau}\rho^k=-i[H_0,\rho^k]-\tfrac{1}{2}[\Gamma,\rho^k]_+ + \begin{bmatrix} 1 & 0 \\ 0 & 0 \end{bmatrix}\frac{d}{d\tau}\left[1-\sum_{i=0}^{k-1}\mathrm{Tr}\rho^i\right], \tag{20}$$

with

$$\rho^k(\tau=0)=0 \quad (k>0) .$$

These equations can be written in a much simpler form by replacing each of the 2×2 density matrices ρ^k by a vector $\tilde{\rho}^k=(\rho^k{}_{11},\rho^k{}_{12},\rho^k{}_{21},\rho^k{}_{22})^T$, where T indicates the transpose. The system of Eqs. (19) and (20) then becomes

$$\frac{d}{d\tau}\tilde{\rho}^0=A\tilde{\rho}^0 \tag{21a}$$

and

$$\frac{d}{d\tau}\tilde{\rho}^k=A\tilde{\rho}^k+B\tilde{\rho}^{k-1} \quad (k>0) , \tag{21b}$$

with

$$A=\begin{bmatrix} 0 & \frac{i\Delta_1}{2} & \frac{-i\Delta_1}{2} & 0 \\ \frac{i\Delta_1}{2} & \frac{-\Gamma_d}{2}-i\sigma & 0 & \frac{-i\Delta_1}{2} \\ \frac{-i\Delta_1}{2} & 0 & \frac{-\Gamma_d}{2}+i\sigma & \frac{i\Delta_1}{2} \\ 0 & \frac{-i\Delta_1}{2} & \frac{i\Delta_1}{2} & -\Gamma_d \end{bmatrix} \tag{21c}$$

and

$$B=\begin{bmatrix} 0 & 0 & 0 & \Gamma_d \\ 0 & 0 & 0 & 0 \\ 0 & 0 & 0 & 0 \\ 0 & 0 & 0 & 0 \end{bmatrix}. \tag{21d}$$

These equations can be solved for any finite number of subsystems since a given subsystem is coupled only to subsystems above it. The result for eight subsystems with $\sigma=0$ (on resonance) and $\Delta_1=\Gamma_d$, computed numerically, is shown in Fig. 4. Plotting the trace of the density matrix for each subsystem, one can follow the propagation of probability density down the washboard, noting that there is a distribution of rates of motion due to the stochastic nature of the decay process. This distribution ap-

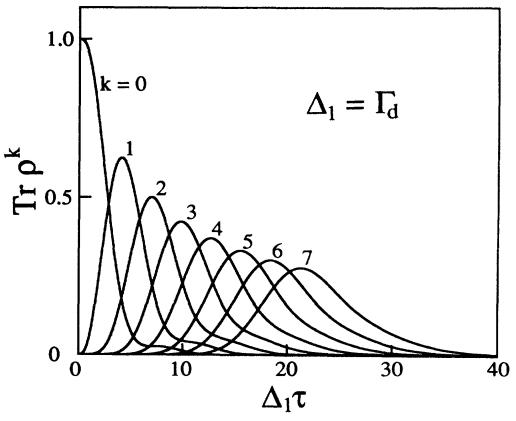

FIG. 4. Propagation of probability density through the first eight subsystems ($k=0$ through $k=7$). Shown is the time dependence of the traces of the density matrix in each subsystem for $\Delta_1=\Gamma_d$. The time dependence scales inversely with Δ_1 and is thus plotted as a function of $\Delta_1\tau$.

pears as a spreading of the quantities $\mathrm{Tr}\rho^k(\tau)$ in τ as k increases.

We are now in a position to estimate the expectation value of the rate of motion down the potential. The expectation value for the phase $\langle\phi\rangle$ is given by

$$\frac{\langle\phi\rangle}{2\pi}=\sum_{k=1}^{\infty}k(\rho^k{}_{11}+\rho^{k-1}{}_{22})\ . \tag{22}$$

We find that, after an initial transient on the order of the transition time out of the $k=0$ subsystem, $\langle\phi\rangle$ is linear in τ. We define γ as the slope of $\langle\phi\rangle/2\pi$ in this region, that is, $(d/d\tau)\langle\phi\rangle/2\pi\rightarrow\gamma$ as $\tau\rightarrow\infty$. We take γ to be the rate of the steady motion down the potential, as the initial deviation from this steady motion is simply an artifact of the somewhat artificial initial conditions. The time derivative of $\langle\phi\rangle/2\pi$ is

$$\begin{aligned}\frac{d}{d\tau}\frac{\langle\phi\rangle}{2\pi}&=\sum_{k=1}^{\infty}k\,\mathrm{Tr}\frac{d}{d\tau}\rho^k+\sum_{k=0}^{\infty}\frac{d}{d\tau}\rho^k{}_{22}\\&=\sum_{k=1}^{\infty}k\xi\cdot(A\tilde{\rho}^k+B\tilde{\rho}^{k-1})+\sum_{k=0}^{\infty}\frac{d}{d\tau}\rho^k{}_{22}\\&=\sum_{k=0}^{\infty}\Gamma_d\rho^k{}_{22}+\sum_{k=0}^{\infty}\frac{d}{d\tau}\rho^k{}_{22}\ ,\end{aligned} \tag{23}$$

where the inner product $\xi\cdot\tilde{\rho}$ of $\xi=(1,0,0,1)$ and a vector $\tilde{\rho}$ produces the trace of the associated matrix ρ.

Rather than solve the entire system of Eqs. (21) to evaluate this expression, we find that the quantity (23) can be extracted from the following simple construction. Defining

$$\tilde{\rho}^{\,\mathrm{tot}}\equiv\sum_{k=0}^{\infty}\tilde{\rho}^{\,k}\ , \tag{24}$$

which is the sum of all the subsystem density matrices (in vector form), and summing the system of Eqs. (21) over all k, we can write

$$\begin{aligned}&\frac{d}{d\tau}\tilde{\rho}^{\,\mathrm{tot}}=\tilde{A}\tilde{\rho}^{\,\mathrm{tot}}\ ,\\&\tilde{A}=A+B\ ,\\&\tilde{\rho}^{\,\mathrm{tot}}(0)=(1,0,0,0)^T\ .\end{aligned} \tag{25}$$

This system, which we refer to as the reduced system, is shown schematically in Fig. 5. Physically it corresponds to taking the probability density as it leaves a subsystem and returning it incoherently to the ground state of the same subsystem. It is in fact the linear superposition of the subsystems, which obey the same equation of motion with the exception of the source terms. Because $\xi\cdot\tilde{A}=0$ the trace is conserved in the reduced system; the constraint that the particle remain within the set of ground states and first excited states corresponds to probability density remaining in the two states of the reduced system.

The reduced system has the steady-state solution (in matrix form)

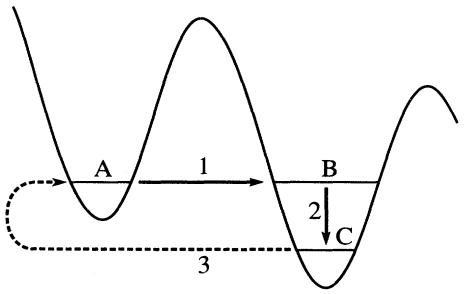

FIG. 5. Schematic representation of the reduced system for $l_{\max}=2$. The reduced system consists of states A and B, which are coupled by the coherent transition (1). Probability density leaves state B by decay (2) to state C of the full system. In the reduced system this density is incoherently reintroduced at state A, as shown by the dotted arrow (3).

$$\lim_{\tau\rightarrow\infty}\rho^{\mathrm{tot}}=\frac{1}{\Gamma_d^2+2\Delta_1^2+4\sigma^2}\times\begin{bmatrix}\Gamma_d^2+\Delta_1^2+4\sigma^2 & \Delta_1(i+2\sigma)\\ \Delta_1(-i+2\sigma) & \Delta_1^2\end{bmatrix} \tag{26}$$

giving

$$\gamma=\frac{\Gamma_d\Delta_1^2}{\Gamma_d^2+2\Delta_1^2+4\sigma^2}\ . \tag{27}$$

This result for the overall rate γ is plotted at resonance ($\sigma=0$) as a function of Γ_d in Fig. 6. This expression can be explained intuitively for Γ_d/Δ_1 much less than or much greater than unity. When $\Gamma_d/\Delta_1\ll1$, the limiting process is the decay, and we expect a subsystem to undergo many oscillations between its two states before decaying, spending half its time in the excited state. As the decay rate of this excited state is Γ_d, we obtain $\gamma=\Gamma_d/2$ in this limit. In the opposite limit, $\Gamma_d/\Delta_1\gg1$, the resonant tunneling is the limiting process. Decay occurs shortly

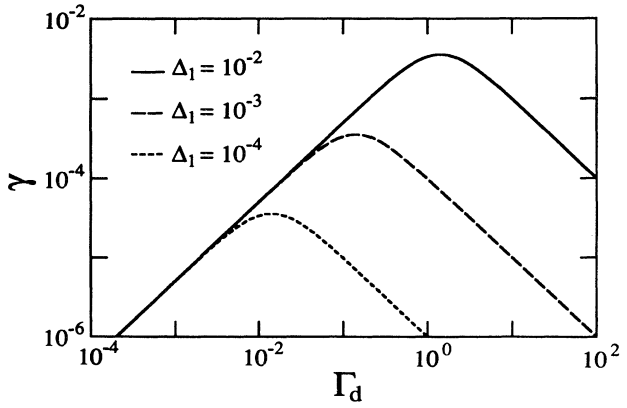

FIG. 6. Rate of motion γ down the washboard at resonance as a function of the decay rate Γ_d for typical interwell couplings of $\Delta_1=10^{-2}$, 10^{-3}, and 10^{-4}.

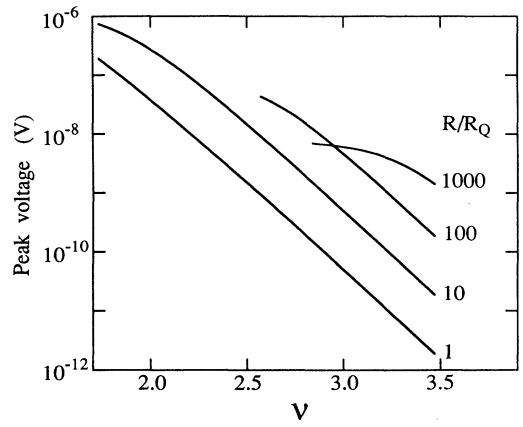

FIG. 7. Maximum voltage developed across the junction by resonant tunneling on the first resonance, plotted as a function of ν for several values of R/R_Q and a plasma frequency $\omega_p/2\pi=10^{10}$ Hz. The curves for $R/R_Q=100$ and 1000 are cut off where $\gamma\tau_{\rm life}=1$ (see text).

after the particle tunnels into the excited state, which is lifetime broadened into a continuous density of states $D(\sigma)=(\Gamma_d/2\pi)/(\sigma^2+\Gamma_d^2/4)$, and the possibility of tunneling back to the ground state is negligible. Fermi's golden rule then applies, giving $\gamma=2\pi|\Delta_1/2|^2D(0)=\Delta_1^2/\Gamma_d$.

The voltage developed across the junction at or near resonance due to this steady motion is then simply

$$V=\Phi_0\omega_p\gamma/2\ , \tag{28}$$

where $\Phi_0=h/2e=2.07\times10^{-15}$ Wb is the flux quantum. Using the dependence (16) of σ on bias current I and treating Δ_1 as a constant, we find that V is Lorentzian-shaped as a function of I, with half width at half maximum

$$\Delta I=\frac{e}{\pi}\omega_p\frac{(\Gamma_d^2+2\Delta_1^2)^{1/2}}{4}\ . \tag{29}$$

We note that ΔI scales with the lifetime broadening width $\Gamma_d/2$ of the excited state when $\Gamma_d\gg\Delta_1$, and with the coupling $\Delta_1/2$ when $\Gamma_d\ll\Delta_1$. We can evaluate the voltage (28) at resonance in terms of the junction parameters ω_p, ν, and R. Using the expression $\Gamma_d=2/(RC\omega_p)$ and writing the capacitance as $C=\pi\nu/\omega_pR_Q$, where $R_Q=\pi\hbar/2e^2=6.45$ kΩ is the quantum of resistance, we obtain $\Gamma_d=2R_Q/\pi\nu R$. Taking this result along with our estimate for Δ_1 and $\omega_p/2\pi=10^{10}$ Hz, we obtain the peak voltage as a function of ν for several ratios of R/R_Q, plotted in Fig. 7.

C. Lifetime of the peak and switching distributions

Next we consider the consequences of additional states in the subsystem and the escape to the free running states. The mixing of the states within a subsystem implies that there is a nonzero probability of finding the particle in one of the states other than Ψ_{k1} and Ψ_{k2}, and in particular, in one of the states $\Psi_{kl_{\rm max}}$ that is separated from the set of free running states by a single barrier, allowing escape of the particle to these states via tunneling. These additional states and the tunneling process can be included by a simple extension of the method used above. The additional states are included in the basis for the subsystem. The tunneling, which is an incoherent process characterized by a constant rate, is added as an imaginary energy term in the energy of the states $\Psi_{kl_{\rm max}}$ analogous to the treatment of decay.

This treatment, unfortunately, cannot be continuously applied over the entire range of ν, as it is based on the assumption of the existence of an integral number of distinct bound states in a subsystem, and this is not always a very sharply defined quantity. Using Eqs. (5), (7), and (11) for the energy levels, we estimate that near resonance there are two bound states in a subsystem for ν roughly between 1.7 and 2.6, and three states for ν between 2.6 and 3.5. More realistically, however, for $\nu\approx2.6$ the "third state" is actually a continuous density of states which are hybrids combining a localized state and the free running states. In this region of ν the present treatment is not applicable. However, we may apply the method with confidence for the intermediate values of ν in the two ranges $1.7<\nu<2.6$ and $2.6<\nu<3.5$ and extrapolate these results into the intermediate region $\nu\approx2.6$.

In each of these two ranges of ν we estimate the tunneling rate from the state $\Psi_{kl_{\rm max}}$ into the continuum of free states using the WKB method. The expression for this rate, expressed in units of $\omega_p/2$ and denoted by $\Gamma_{l_{\rm max}}^{\rm WKB}$, is

$$\Gamma_{l_{\rm max}}^{\rm WKB}=\frac{1}{\pi}G(l_{\rm max})\exp(-2I_{l_{\rm max}})\ , \tag{30}$$

where I and G are given by Eqs. (14) and (15), respectively.

The terms representing coherence in the equations of motion (19) and (20) remain unchanged in form. However, the matrices H_0 and Γ appearing in these terms must be modified to include the additional states and tunneling rates. For the case of two states per subsystem ($1.7<\nu<2.6$), H_0 is as before, while Γ becomes

$$\Gamma=\begin{bmatrix}0 & 0\\ 0 & \Gamma_d+\Gamma_2^{\rm WKB}\end{bmatrix}\ . \tag{31}$$

In the case of three states per subsystem ($2.6<\nu<3.5$), we include in the subsystem basis the state Ψ_{k3}, which has energy ε relative to the average of the energies of states Ψ_{k1} and Ψ_{k2}. This energy is given by

$$\varepsilon=3-3\pi s\nu-\frac{3s^2}{4}-\frac{5}{4\nu}-\frac{15}{32\nu^2} \tag{32}$$

to second order in $1/\nu$. Defining $\Delta_2/2\equiv H_{0,1,1,2}$, we obtain

$$H_0=\begin{bmatrix} \frac{\sigma}{2} & \frac{\Delta_1}{2} & 0 \\ \frac{\Delta_1}{2} & \frac{-\sigma}{2} & \frac{\Delta_2}{2} \\ 0 & \frac{\Delta_2}{2} & \varepsilon \end{bmatrix},$$

$$\Gamma=\begin{bmatrix} 0 & 0 & 0 \\ 0 & \Gamma_d & 0 \\ 0 & 0 & 2\Gamma_d+\Gamma_3^{\mathrm{WKB}} \end{bmatrix}. \tag{33}$$

We note that $|\sigma|+|\varepsilon| \gg \Delta_1, \Delta_2$, which implies that at most two of the states are strongly mixed at a given bias current. This tends to suppress the escape rate by reducing the probability of several resonant tunneling events occurring in succession. Also we point out that we have taken the decay from Ψ_{k3} to $\Psi_{k+1,2}$ to have twice the rate as that from Ψ_{k2} to $\Psi_{k+1,1}$. This is exactly true in the case of the harmonic oscillator[19] and we expect it to be a reasonable approximation in the present case.

The source terms in Eq. (20) must be modified to include only the contributions of the decay process. This is most easily done after the transformation from matrices to column vectors has been performed. For example, in the case of two states per well, the source matrix B given in Eq. (21d) remains unchanged, whereas in matrix A, given by Eq. (21c), Γ_d is replaced by $\Gamma_d+\Gamma_2^{\mathrm{WKB}}$.

Again we can transform the coupled equations of motion for the entire set of subsystems to the equation of motion

$$\frac{d}{d\tau}\tilde{\rho}^{\mathrm{tot}}=\tilde{A}\tilde{\rho}^{\mathrm{tot}} \tag{34}$$

for a single reduced system, which is identical in form to Eq. (25) except that now $\tilde{A}$ is either a 4×4 or 9×9 matrix.

The reduced system (34) can be solved numerically. As asserted previously, we find that the motion studied in part B of this section is only weakly perturbed, except when ν is small and the resistance R is large. For short times the elements of the density matrix reach approximately the same steady-state values as they had before the inclusion of escape. For longer times, however, we find that each of the elements undergoes a slow exponential decay, and the trace is no longer conserved. This decay of the trace corresponds to the escape of probability density via tunneling into the free running states.

The full solution of Eq. (34) is a linear combination of solutions, each containing a factor $\exp(\lambda\tau)$ in the time dependence, where λ is one of the eigenvalues of $\tilde{A}$. When escape is not included ρ^{tot} has a steady-state solution, which corresponds to the eigenvalue 0. When escape is included, this eigenvalue is shifted slightly in the negative direction along the real axis, and is associated with the slow exponential decay of the trace. It is the negative value of this eigenvalue that we take as the overall escape rate, and the reciprocal of this rate τ_{life} gives the (dimensionless) lifetime of the resonant peak

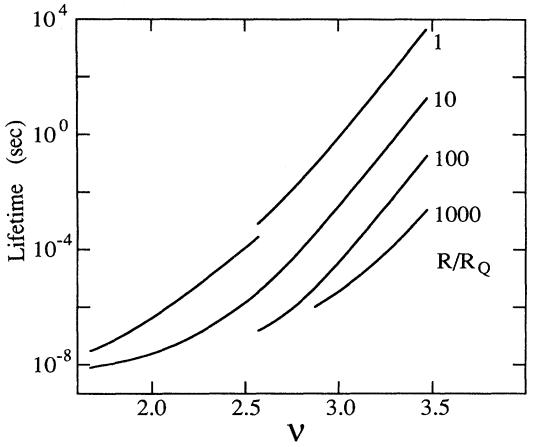

FIG. 8. Lifetime t_{life} of the first voltage peak on resonance $I=I_1^{\mathrm{res}}$ before escape occurs, computed with the same set of junction parameters as in Fig. 7.

structure. We note that one obtains meaningful results from this method only when the product $\gamma\tau_{\mathrm{life}}$ is greater than unity. This quantity is an estimate of the number of interwell transitions the particle makes before escaping, and when this number is less than one the coupling to the continuum is so strong that the bound-state approximation becomes invalid and an alternative approach must be used.

We have calculated both the lifetime $t_{\mathrm{life}}=2\tau_{\mathrm{life}}/\omega_p$ at the resonance $I=I_1^{\mathrm{res}}$ and the escape rate t_{life}^{-1} as a function of bias current near the resonance, in each case using the same set of parameters as we used in calculating the magnitude of the voltage peak. The lifetimes are shown in Fig. 8, and the escape rates are shown in Figs. 9 and 10. In both the lifetime and the escape rates we find small discontinuities at $\nu=2.6$ which arise between the two and three-state treatments. This is not alarming con-

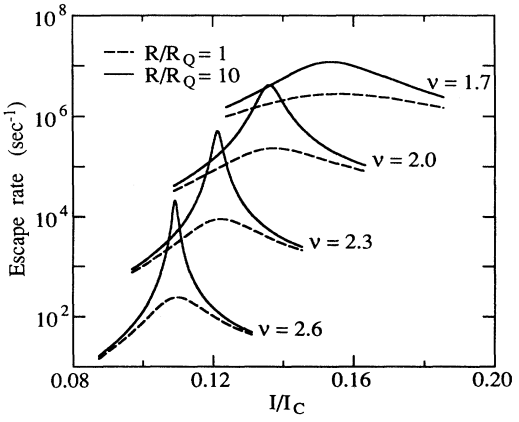

FIG. 9. Distribution of rates at which the junction switches to the normal state as a function of bias current for the case of two states per well, plotted for $\nu=1.7$, 2.0, 2.3, and 2.6 and $R/R_Q=1$ and 10.

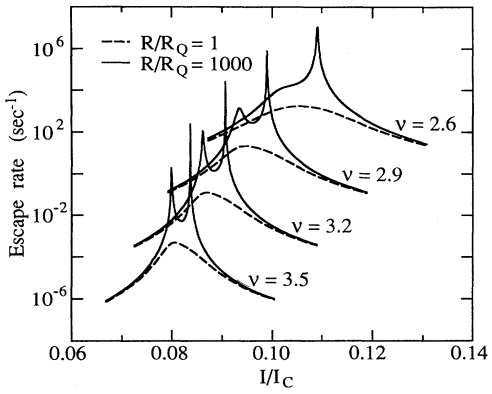

FIG. 10. Distribution of rates at which the junction switches to the normal state as a function of bias current for the case of three states per well, plotted for $\nu=2.6$, 2.9, 3.2, and 3.5, and $R/R_Q=1$ and 1000.

sidering the discontinuity inherent in the two methods. The match is in fact remarkably good when we note that small changes in Δ_1, Δ_2, $\Gamma_2^{\rm WKB}$, and $\Gamma_3^{\rm WKB}$ can greatly increase or decrease the discontinuities, and perhaps better estimates of these quantities would further smooth the transition.

IV. DISCUSSION AND CONCLUSIONS

We have investigated the phenomenon of resonant tunneling that occurs in small Josephson junctions. In this section we discuss the prospects of experimental observation of the primary signatures of resonant tunneling, namely voltage peaks on the supercurrent branch of the current-voltage characteristic and the distinctive distribution of rates at which the junction switches to the normal state.

We focus our attention first on the voltage peaks. In Fig. 7 we see that the magnitude of the voltage is on the order of 1 μV for $\nu=1.7$ and decreases exponentially with increasing ν, becoming rather small (10^{-12} to 10^{-9} V) for $\nu=3.5$. On the other hand, the lifetime of the voltage peak ranges from 10^{-8} to 10^{4} sec, as we see in Fig. 8. Evidently, in choosing values of ν and R one must balance between measuring an extremely small signal of lengthy duration and a larger signal of extremely short duration. In order to analyze this apparent trade-off, we construct a figure of merit η which is the estimated voltage signal at resonance divided by the square root of a measurement bandwidth that we take to be the inverse of the estimated lifetime. We obtain values for η between 10^{-12} and 10^{-10} V Hz$^{-1/2}$ for the entire range $1.7\leq\nu\leq3.5$ and $1\leq R/R_Q\leq1000$. Since the quietest semiconductor amplifiers have a typical voltage noise of 10^{-9} V Hz$^{-1/2}$ this result implies that the use of such amplifiers for the direct observation of the voltage peaks is most certainly ruled out. However, a more sophisticated method exploiting signal averaging techniques may reveal this structure.

Thus, it appears that the most readily observable effect arising from resonant tunneling is the distribution of rates at which the junction switches to the normal state, shown in Figs. 9 and 10. The most unusual feature of these distributions is that they are nonmonotonic in the bias current, in contrast to those where switching is caused by thermal activation or macroscopic quantum tunneling. Peaks occur in the escape rate for bias currents at the resonance values. In the case of two states per well (Fig. 9) a single peak appears, corresponding to resonance between states Ψ_{k1} and Ψ_{k2}. In the case of three states per well (Fig. 10), additional smaller peaks appear for slightly smaller bias currents, corresponding to resonances between states Ψ_{k1} and Ψ_{k3} and states Ψ_{k2} and Ψ_{k3}. The former is almost as pronounced as the primary resonance peak, while the latter is very small and cannot be seen on the scale of Fig. 10. With the exception of this small peak, which is largest for $R/R_Q\approx100$, we find in general these peaks are most pronounced for the cases of low damping (high resistance) because the particle spends more time in the excited states $\Psi_{kl_{\rm max}}$ and therefore has a higher probability of escaping through the final barrier to the free states. The observation of these peaks in the distribution of switching rates would be a direct confirmation of the existence of resonant tunneling in Josephson junction dynamics. Measurement of the distribution should be experimentally realizable using existing techniques,[20] although construction of a junction in an environment presenting an impedence $R\gg R_Q$ at the plasma frequency may present a difficulty.

It should be noted that measurements already performed on small capacitance junctions[21] have shown switching currents lower than the value I_C deduced from the Ambegaokar-Baratoff prediction; this reduction may be related to resonant tunneling between localized states. Before making quantitative comparisons, however, one must consider the effects of current noise and construct an experimental configuration in which the effects of external circuitry can either be minimized or quantitatively taken into account.

Finally, it is also apparent from our results that in the region where ν is small and the resistance is large, the escape rate is rather high and the particle makes no more than a few transitions to lower subsystems before escaping. Thus, as one reduces the value of ν, for bias currents corresponding to the resonance condition we expect Bloch oscillations to be suppressed because of escape to the voltage state.

ACKNOWLEDGMENTS

We are indebted to Professor D. S. Rokhsar for helpful suggestions on parts of the calculations and for a critical reading of the manuscript. One of us (A.N.C.) acknowledges support from IBM. This work was supported by the Director, Office of Energy Research, Office of Basic Energy Sciences, Materials Sciences Division of the U.S. Department of Energy under Contract No. DE-AC03-76SF00098.

[1]A. J. Leggett, Prog. Theor. Phys. (Suppl.) **69**, 80 (1980); *Essays in Theoretical Physics in Honour of Dirk Ter Haar* (Pergamon, Oxford, 1984), p. 95.
[2]W. C. Stewart, Appl. Phys. Lett. **12**, 277 (1968); D. E. McCumber, J. Appl. Phys. **39**, 3133 (1968).
[3]J. M. Martinis, M. H. Devoret, and J. Clarke, Phys. Rev. B **35**, 4682 (1987).
[4]R. V. Voss and R. A. Webb, Phys. Rev. Lett. **47**, 265 (1981); S. Washburn, R. A. Webb, R. F. Voss, and S. F. Faris, *ibid.* **54**, 2712 (1985).
[5]L. D. Jackel, J. P. Gordon, E. L. Hu, R. E. Howard, L. A. Fetter, D. M. Tennant, R. W. Epworth, and J. Kurkijarvi, Phys. Rev. Lett. **47**, 697 (1981).
[6]A. N. Cleland, J. M. Martinis, and J. Clarke, Phys. Rev. B **37**, 5950 (1988).
[7]D. Esteve, J. M. Martinis, C. Urbina, E. Turlot, and M. H. Devoret, Phys. Scr. **T29**, 121 (1989).
[8]K. K. Likharev, *Dynamics of Josephson Junctions and Circuits* (Gordon and Breach, New York, 1986).
[9]N. Hatakenaka and S. Kurihara, Solid State Commun. **64**, 943 (1987).
[10]R. F. Kazarinov and R. A. Suris, Fiz. Tekh. Poluprovodn. **6**, 148 (1972) [Sov. Phys. Semicond. **6**, 120 (1972)]; L. L. Chang, L. Esaki, W. E. Howard, and R. Ludeke, J. Vac. Sci. Technol. **10**, 655 (1973).
[11]K. K. Likharev and A. B. Zorin, J. Low Temp. Phys. **59**, 347 (1985).
[12]D. V. Averin and K. K. Likharev, in *Quantum Effects in Small Disordered Systems,* edited by B. L. Altschuler, P. A. Lee, and R. A. Webb (Elsevier, Amsterdam, to be published).
[13]J. Kondo, in *Superconducting Materials,* edited by S. Nakajima and H. Fukuyama (Publication office of the Japanese Journal of Applied Physics, Tokyo, 1988), p. 214.
[14]N. Hatakenaka and S. Kurihara, Solid State Commun. **68**, 131 (1988).
[15]A. V. Zhuravlev and A. B. Zorin, Fiz. Nizk. Temp. **16**, 184 (1990) [Sov. J. Low Temp. Phys. (to be published)].
[16]A. O. Caldeira and A. J. Leggett, Ann. Phys. (N.Y.) **149**, 374 (1983).
[17]V. Ambegaokar and A. Baratoff, Phys. Rev. Lett. **10**, 486 (1963).
[18]*Handbook of Mathematical Functions,* edited by M. Abramowitz and I. A. Stegun (Dover, New York, 1969), Chap. 20.
[19]D. Esteve, M. H. Devoret, and J. M. Martinis, Phys. Rev. B **34**, 158 (1986).
[20]T. A. Fulton and L. N. Dunkleburger, Phys. Rev. B **9**, 4760 (1974).
[21]R. H. Ono, M. W. Cromar, R. L. Kautz, R. J. Soulen, J. H. Colwell, and W. E. Fogle, IEEE Trans. Magn. **MAG-23**, 1670 (1987); M. Iansiti, A. T. Johnson, W. F. Smith, H. Rogalla, C. J. Lobb, and M. Tinkham, Phys. Rev. Lett. **59**, 489 (1987).